The AAPS Journal (2019) 21: 18
DOI: 10.1208/s12248-018-0289-3

Research Article

Tumor-Targeted Chemoimmunotherapy with Immune-Checkpoint Blockade for Enhanced Anti-Melanoma Efficacy

Man Li,[1] Yuting Yang,[1] Chaoqun Xu,[2] Jiaojie Wei,[1] Yingke Liu,[3] Xingli Cun,[1] Qianwen Yu,[1] Xian Tang,[1] Sheng Yin,[1] Zhirong Zhang,[1] and Qin He[1,4]

Received 31 August 2018; accepted 17 December 2018; published online 11 January 2019

ABSTRACT. Chemoimmunotherapy with chemotherapeutics and immunoadjuvant inhibits tumor growth by activating cytotoxic T cells. However, this process also upregulates the expression of PD-1/PD-L1 and consequently leads to immune suppression. To maximize the anti-tumor immune responses and alleviate immunosuppression, PD-L1 antibody was combined with paclitaxel (PTX) and the immunoadjuvant α-galactosylceramide (αGC), which were coencapsulated into pH-sensitive TH peptide-modified liposomes (PTX/αGC/TH-Lip) to treat melanoma and lung metastasis. Compared to treatment with PD-L1 antibody or PTX/αGC/TH-Lip alone, the combination of PD-L1 antibody and PTX/αGC/TH-Lip further elevated the tumor-specific cytotoxic T cell responses and promoted apoptosis in tumor cells, leading to enhanced anti-tumor and anti-metastatic effects. In adoptive therapy, PD-L1 antibody further alleviated immunosuppression and enhanced the anti-tumor effect of $CD8^+$ T cells. The combination of PD-L1 antibody and chemoimmunotherapy PTX/αGC/TH-Lip provides a promising strategy for enhancing treatment for melanoma and lung metastasis.

KEY WORDS: α-galactosylceramide; chemo-immunotherapy; combined strategy; immunosuppression; PD-L1 antibody.

INTRODUCTION

Although traditional cancer treatments such as chemotherapy and surgery suppress the development of tumor cells, the problems of recurrence and chemoresistance remain great challenges (1). In recent decades, the combination of chemotherapy and immunotherapy has shown great potential for eliminating cancer (2). The direct killing of tumor cells mediated by chemotherapy such as paclitaxel and doxorubicin produces tumor-associated antigens or immunogentic cell death (ICD) (3), which is further cross-presented by dendritic cells and macrophages on MHC class I molecules and initiates $CD8^+$ T cell responses. Various immunoadjuvants have been applied in combination with chemotherapy to enhance the function of antigen-presenting cells (APCs), including Toll-like receptors (TLR) (4), cytokines such as granulocyte-macrophage colony-stimulating factor (GM-CSF) and interleukin-2 (IL-2) (5,6), functional polymers (7,8), and glycolipid ligands. α-Galactosylceramide (αGC), a common glycolipid ligand presented on CD1d-expressing APCs, is able to activate natural killer T cells (NK T cells) and consequently activate $CD8^+$ T cells, natural killer (NK) cells, and APCs, which bridge the innate and adaptive immune response and exert considerable influence on the outcomes of immunotherapy (9). Upon activation of NK T cells, downstream NK cells and $CD8^+$ T cells also lead to massive production of Th 1-type cytokine interferon-γ (IFN-γ), which is crucial for αGC-mediated anti-tumor responses as well as antigen presentation.

Tumor-targeted drug delivery systems have exhibited promising results in cancer therapy (10). In our previous studies, PTX and immunoadjuvant αGC were successfully encapsulated in tumor-targeting liposomes mediated by a charge-reversal cell-penetrating peptide (AGYLLGHINLHHLAHL(Aib)HHIL-Cys, TH) (11). The PTX/αGC coloaded liposome (PTX/αGC/TH-Lip) exhibited good serum stability and enhanced cellular internalization. After intravenous injection, PTX/αGC/TH-Lip not only leads to direct tumor killing but also initiates immune responses by facilitating the NK T cell maturation and antigen

Electronic supplementary material The online version of this article (https://doi.org/10.1208/s12248-018-0289-3) contains supplementary material, which is available to authorized users.

[1] Key Laboratory of Drug Targeting, Ministry of Education, West China School of Pharmacy, Sichuan University, No. 17, Section 3, Southern Renmin Road, Chengdu, 610041, People's Republic of China.
[2] Sichuan Academy of Chinese Medicine Science, Chengdu, 610041, People's Republic of China.
[3] West China School of Stomotology, Sichuan University, Chengdu, 610041, People's Republic of China.
[4] To whom correspondence should be addressed. (e–mail: qinhe@scu.edu.cn)

presentation. Subsequently, the αGC-loaded liposome favors Th1 development via IFN-γ secretion, exhibiting a different cytokine release pattern and stimulating the anti-tumor cellular immunity mediated by cytotoxic T lymphocytes (CTLs). The combination of αGC and PTX initiated efficient anti-tumor immune responses.

Nevertheless, the high IFN-γ level in the tumor microenvironment also upregulates immune inhibition signals and impairs the cytotoxicity of $CD8^+$ T cells. Programmed cell death protein 1 (PD-1) or cytotoxic T lymphocyte antigen-4 (CTLA-4) plays a critical role in the maintenance of peripheral tolerance and limits the damage to normal tissue during inflammatory responses (12). Though PD-1 expression is considered the first marker of T cell activation (13), the PD-1/PD-L1 axis impairs T cell receptor (TCR) signaling and CD28 costimulation (14), which is associated with a loss of T cell functions. Moreover, the expression of PD-L1 is regulated by proinflammatory cytokines. The secretion of IFN-γ in the tumor microenvironment upregulated the expression of immune checkpoints such as PD-L1 or CTLA-4 in tumor cells and infiltrating immune cells, which generated an immunosuppressive signal by binding with their ligands and formed an immunosuppressive tumor microenvironment (15–17). This phenomenon may explain the failure of many immunotherapies that aimed to directly stimulate the anti-tumor immune response. Interestingly, the inhibition of the PD-1/PD-L1 pathway has shown great potential in cancer treatment both in clinical studies and in preclinical studies (18). CTLA-4 antibody and PD-1/PD-L1 antibody have already been proven by the U.S. Food and Drug Administration (FDA) in the treatment of different types of cancers such as Hodgkin's lymphoma, non-small cell lung cancer, and melanoma (19–21).

Though these checkpoint blockade antibodies showed excellent clinical yield in cancer treatment, a large number of patients do not respond to such single-agent therapy (22), emphasizing the need for combined therapy. The combination of PD-1/PD-L1 inhibitors with cytotoxic chemotherapy, radiotherapy, and photodynamic therapy has been reported (23,24). Facing the problem of enhanced IFN-γ levels induced by PTX and αGC-based chemo-immunotherapy, we proposed a hypothesis that the combination of PD-L1 antibody and PTX/αGC/TH-Lip could alleviate the immunosuppression of cytotoxic T cells and facilitate the anti-tumor immune response, which would eventually augment the anti-tumor effect. To prove this concept, B16F10 melanoma-bearing and melanoma lung metastasis models were established. The upregulation of IFN-γ after PTX/αGC/TH-Lip was identified. After intravenous injections of PTX/αGC/TH-Lip and PD-L1 antibody, the anti-tumor and anti-metastatic effects were evaluated, and the mechanisms involved in this process were explored.

MATERIALS AND METHODS

Materials, Cells, and Animals

L-α-phosphatidylcholine from soybean (SPC) was purchased from Shanghai Taiwei Chemical Company (Shanghai, China). Cholesterol was obtained from Chengdu Kelong Chemical Company. TH peptide with a terminal cysteine (AGYLLGHINLHHLAHL(Aib)HHIL-Cys) was synthesized by China Peptides Co. Ltd. (Shanghai, China). DSPE-PEG_{2000} and DSPE-PEG_{2000}-Mal were purchased from Avanti Polar Lipids (USA). Paclitaxel was purchased from Meilun Pharmaceutical Co. Ltd. (Dalian, China). αGC (KRN7000) was obtained from Cayman Chemical (Ann Arbor, Michigan, USA). Anti-PD-1 antibody was obtained from Novus (USA). Mouse IFN-γ, IL-6, and IL-17 Ready-Set-Go! enzyme-linked immunosorbent assay (ELISA) kits were purchased from eBioscience (USA). B16F10 murine melanoma cells were obtained from the Cell Bank at the Chinese Academy of Science (Shanghai, China). Cells were maintained in Dulbecco's modified Eagle's medium (DMEM) supplemented with 10% fetal bovine serum (FBS; Gibco, USA), 100 U/mL streptomycin, and 100 U/mL penicillin (Beyotime, Beijing, China). Female C57BL/6 (6- to 8-week-old) mice were purchased from Dashuo Biotechnology (Chengdu, China) and housed in a specific pathogen-free and temperature-controlled facility. All animal experiments were performed under the Guidelines for the Care and Use of Laboratory Animals of Sichuan University and were approved by the experimental animal administrative committee of Sichuan University.

Formulation and Characterization of PTX/αGC Coloaded Liposomes

TH peptide-modified liposomes loaded with PTX and αGC were formulated as described in previous reports (11). Briefly, the Cys-TH peptide was conjugated with DSPE-PEG_{2000}-Mal via the Michael addition reaction. TH-modified liposomes were prepared with cholesterol/SPC/DSPE-PEG_{2000}/DSPE-PEG_{2000}-TH (molar ratio = 33:59:2:6) by the thin film hydration method. After evaporation of organic solvent (chloroform/methanol = 2:1), the lipid film was hydrated with HEPES buffer (pH 7.4). Liposomes loaded with PTX or αGC alone or coloaded with both PTX and αGC were prepared by adding PTX and/or αGC before evaporation. The mean particle sizes and ζ potentials of PTX/αGC/TH-Lip at pH 7.4 and pH 6.0 were measured by a Malvern Zetasizer Nano Instrument (Malvern Instruments Ltd., UK). The morphology of PTX/αGC/TH-Lip was analyzed by transmission electron microscopy (TEM, H-600, Hitachi, Japan). The encapsulation efficiency and release profiles of PTX at pH 7.4 and pH 6.0 were analyzed by high-performance liquid chromatography (HPLC, Agilent 1200 series, CA). The stability of liposomes was determined by analyzing the optical density after incubation with fetal bovine serum (FBS).

In Vivo Secretion of IFN-γ After Treatment with PTX/αGC-TH-Lip

A B16F10 melanoma-bearing mouse model was established by subcutaneous injection of B16F10 cells (5×10^5 cells) into C57/BL6 mice. To identify the upregulation of IFN-γ after treatment with chemoimmunotherapy, melanoma-bearing mice were randomized into four groups ($n = 3$) and treated intravenously with PTX/αGC/TH-Lip, αGC/TH-Lip, free PTX, and αGC or HEPES buffer when the tumor volume reached 100 mm^3. The doses of PTX and αGC were 0.3 mg/mL and 25 μg/mL, respectively. Serum was collected from each mouse at 24 and 48 h after administration. The IFN-γ level in serum was determined by ELISA.

Upregulation of PD-L1 Under the Condition of High IFN-γ

The upregulation of PD-L1 in the presence of high concentrations of IFN-γ was tested both *in vitro* and *in vivo*. B16F10 cells were seeded in six-well plates and incubated at 37°C overnight. INF-γ (200 U/mL) was added and incubated for 24 or 48 h. Cells treated without IFN-γ were used as a control. After incubation, the cells were trypsinized and washed with PBS. Then, the cells were stained with FITC-labeled anti-PD-L1 antibody. The upregulation of PD-L1 on B16F10 was analyzed by flow cytometry (Cytomics^{TM} FC 500, Beckman Coulter, USA).

To determine the in vivo upregulation of PD-L1, C57BL/6 mice were inoculated with B16F10 cells as mentioned above. Mice were randomized into four groups when the tumor volume reached 100 mm^3 and were administered PTX/αGC/TH-Lip (PTX 0.3 mg/mL, αGC 25 μg/mL), αGC/TH-Lip, free PTX, and αGC or HEPES buffer via intravenous injection. Mice received injections every 2 days for a total of three injections. Seven days after the last administration, mice were sacrificed by cervical dislocation. The tumor tissues were isolated, hydrated, and fixed with 4% paraformaldehyde. Then, the tissues were embedded in paraffin and sectioned, followed by immunohistochemical staining with anti-PD-L1 antibody. The upregulation of PD-L1 was observed with an inverted microscope (Leica, Germany).

The Anti-Tumor Effect of the Combined Treatment with PTX/αGC-TH-Lip and Anti-PD-L1 Antibody

The anti-tumor effect of combination therapy with PTX/αGC-TH-Lip and anti-PD-L1 antibody was explored in a B16F10 melanoma-bearing mouse model. To extensively analyze the anti-tumor effects, mice were intravenously administered PTX/αGC-TH-Lip, PD-L1 antibody, PTX/αGC-TH-Lip+ PD-L1 antibody, or HEPES buffer when the tumor volume reached 100 mm^3 (seven mice/group). PD-L1 antibody (5 mg/kg) was injected intravenously 48 h after administration of PTX/αGC-TH-Lip. All mice received 3 cycles of administrations with intervals of 2 days. The tumor volumes were monitored every other day. One week after the last administration, the mice were sacrificed by cervical dislocation. To determine the apoptosis levels, the tumor tissues were isolated for paraffin sections followed by hematoxylin & eosin (H&E) staining or terminal deoxynucleotidyl transferase dUTP nick end labeling (TUNEL) staining.

To study the survival of tumor-bearing mice after a combination of drug-loaded liposomes and PD-L1 antibody, B16F10 melanoma-bearing mice were randomized into seven groups (10 mice/group). Mice were treated with the strategies described above for 4 cycles. The survival of the mice was monitored every day, and Kaplan-Meier survival curves were plotted.

The Anti-Metastatic Effects of the Combined Strategy of PTX/αGC-TH-Lip and Anti-PD-L1 Antibody

The melanoma lung metastasis model was established on day 1 by intravenous injection of lung B16F10 melanoma cells (1×10^6/100 μL) to analyze the anti-metastatic effect of PTX/αGC-TH-Lip in combination with PD-L1 antibody. On day 4, mice were randomized into four groups (five mice per group) and were administered PTX/αGC-TH-Lip, PD-L1 antibody, PTX/αGC-TH-Lip + PD-L1 antibody, or HEPES buffer as previously described. After 4 cycles of administration, mice were sacrificed by cervical dislocation on days 20, 23, and 26 to monitor the lung metastasis. The lungs were isolated, observed, and weighed.

The *Ex Vivo* CTL Response of the Combined Therapy

B16F10 melanoma-bearing mice were established, randomized into two groups (three mice/group), and treated intravenously with PTX/αGC-TH-Lip or HEPES buffer. Two days later, mice were given a second administration. One week after the two injections, the splenocytes were obtained from the mice, and CD8$^+$ T cells were isolated using a CD8$^+$ T cell isolation kit (Miltenyi Biotech, Germany) and further incubated with mitomycin C-treated B16F10 tumor cells or irrelevant C26 cells in the presence of mouse IL-2 (200 U/mL). After 72 h of stimulation, viable CD8$^+$ T cells were used as effector cells and added to B16F10 cells or C26 cells preseeded in 96-well plates, which were used as target cells. The ratios of the effector cells and the target cells were 20:1, 5:1, and 1:1, respectively. In addition, PD-L1 antibody (50 μg/mL) was added to effector cells obtained from mice treated with PTX/αGC-TH-Lip to evaluate the promotion of CTL cytotoxicity. After 6 h of incubation, the supernatant was collected and the cytotoxicity of CTL was analyzed using a lactate dehydrogenase (LDH) assay (Beyotime, China). Untreated B16F10 cells (or C26 cells) were used as a negative control. Target cells treated with cell lysis buffer were used as a positive control. The specific cell lysis ratio was calculated with the following equation: $\text{Specific lysis}\% = (A_{\text{sample}} - A_{\text{negative control}}) / (A_{\text{positive control}} - A_{\text{negative control}}) \times 100\%$.

CTL Adoptive Immunotherapy

The promotion of the cytotoxicity of CD8$^+$ T cells by PD-L1 was also analyzed in vivo in a melanoma model. Tumor-bearing mice were randomized into two groups (five mice/group) and given PTX/αGC-TH-Lip or HEPES buffer. Effector CD8$^+$ T cells were obtained as described above after two administrations and were intravenously administered into another group of B16F10 melanoma-bearing mice (1.5×10^6 cells/mouse). In addition, PD-L1 antibody (5 mg/kg) was combined with CD8$^+$ T cells obtained from PTX/αGC-TH-Lip-treated mice to analyze the promotion of anti-tumor responses. The tumor volumes were monitored every other day, and the overall survival of tumor-bearing mice was calculated using the Kaplan-Meier method.

Preliminary Safety Analysis of the Combined Strategy

To evaluate the in vivo toxicity of the combined therapy, the serum levels of chemokines IL-6 and IL-17a in the serum of mice were determined by ELISA. Tumor-bearing mice were given PTX/αGC-TH-Lip, PTX/αGC-TH-Lip plus PD-L1 antibody, or HEPES buffer. Untreated mice were used as controls. One week after 3 cycles of injections, serum was obtained by retro-orbital puncture. The levels of IL-6 and IL-17a were analyzed by ELISA according to the manufacturer's instructions. Major organs (heart, liver, spleen, lung, and

kidney) were isolated for paraffin sections, and the tissue sections were subjected to H&E staining to evaluate the toxicity to major organs.

Statistical Analysis

All data are presented as the mean ± standard deviation (mean ± SD). Experiments were conducted at least in triplicate unless otherwise noted. Statistical comparisons were performed by analysis of variance (ANOVA) with the Tukey post hoc test for multiple groups. P values < 0.05 were considered indicative of statistical significance.

RESULTS AND DISCUSSION

Characterization of PTX/αGC-TH-Lip

In the acidic tumor microenvironment, the protonation effect of the imidazole ring led to a charge reversal of the TH peptide, which further facilitated the internalization of PTX/αGC-TH-Lip. As shown in Fig. 1a, the particle size was 116 ± 3.7 nm at pH 7.4 and 118 ± 2.6 nm at pH 6.0, which indicated that the particle size was stable at neutral and acidic pH. In contrast, the zeta potential of PTX/αGC-TH-Lip exhibited obvious changes at different pH values. At neutral pH, the zeta potential of PTX/αGC-TH-Lip was −7.3 ± 1.9 mV, while at pH 6.0, an obvious charge reversal was observed and the zeta potential increased to +3.8 ± 0.9 mV. In our previous reports, the cellular uptake of TH peptide-modified liposomes was increased compared to pegylated liposomes (11). The encapsulation efficiency of PTX in TH-modified liposomes was above 90% at both pH 7.4 and pH 6.0 with a sustained release profile (Supporting Information Fig. S1). To test whether these nanoparticles form aggregates in serum, we have analyzed the serum stability of PTX/αGC-TH-Lip in medium containing 50% FBS. The results suggested that PTX/αGC-TH-Lip exhibited good serum stability (Supporting Information Fig. S2).

Histidine has been widely studied for the development of pH-responsive drug delivery systems since it is a major amino acid responsible for the buffering capacity of biological systems. TH peptide (AGYLLGHINLHHLAHL(Aib)HHIL-Cys) is a pH-sensitive cell-penetrating peptide that can be converted to a positive charge due to the protonation of the imidazole ring in the acidic tumor microenvironment. Then, the positively charged TH peptide dramatically increases the cellular internalization and tumor penetration of its payload. In our previous studies, PTX-loaded TH peptide-modified liposomes exhibited obvious tumor suppression. This drug delivery system was also proven to be potent in chemoimmunotherapy by coloading with immunoadjuvants such as αGC. Owing to the enhanced tumor penetration and cellular uptake, stronger anti-tumor immune responses were initiated, and elevated tumor repression was achieved (11).

IFN-γ Was Upregulated in PTX/αGC-TH-Lip-Treated B16F10-Bearing Mice

Chemoimmunotherapy exhibits great potential in suppressing tumor growth. The immunoadjuvant αGC facilitates anti-tumor responses by activating NK T cells and secreting IFN-γ, which further promotes the activation of $CD8^+$ T cells, NK cells, and dendritic cells. We have analyzed the maturation of dendritic cells and activation of NK T cells in tumor-bearing mice after treatment of PTX/αGC-TH-Lip, αGC-TH-Lip, free PTX+αGC, and HEPES buffer. The results showed that PTX/αGC-TH-Lip elicited the highest amount of activated dendritic cells and NK T cells (Supporting Information Fig. S3A–3D). Nevertheless, the secreted IFN-γ in turn upregulates the PD-L1 level in tumor cells. The subsequent binding of PD-L1 to PD-1 helps tumor cells escape immune surveillance by protecting PD-L1-positive tumor cells from $CD8^+$ T cell-mediated lysis and inducing the apoptosis and anergy of T cells (25,26). First, to prove the upregulation of IFN-γ, tumor-bearing mice were treated with PTX/αGC-TH-Lip by intravenous injections. Blood serum was obtained at 24 and 48 h after injection. As shown in Fig. 2a, IFN-γ levels in mice were significantly upregulated as early as 24 h after treatment with free αGC or αGC loaded in TH liposomes. The high level of IFN-γ lasted for 48 h. PTX/αGC-TH-Lip, αGC-TH-Lip, or free PTX and αGC significantly increased the IFN-γ level in serum compared with HEPES buffer treated mice at both 24 and 48 h after treatment ($p < 0.005$). These observations provide the basis for the combination of PD-L1 antibody and PTX/αGC-TH-Lip. Notably, αGC is an immunoadjuvant that activates NK T cells, which is responsible for the production of IFN-γ (27). Upon intravenous injections, due to the existence of NK T cells in the peripheral lymphatic system, free PTX and αGC could activate NK T cells in the peripheral blood and induce the production of IFN-γ.

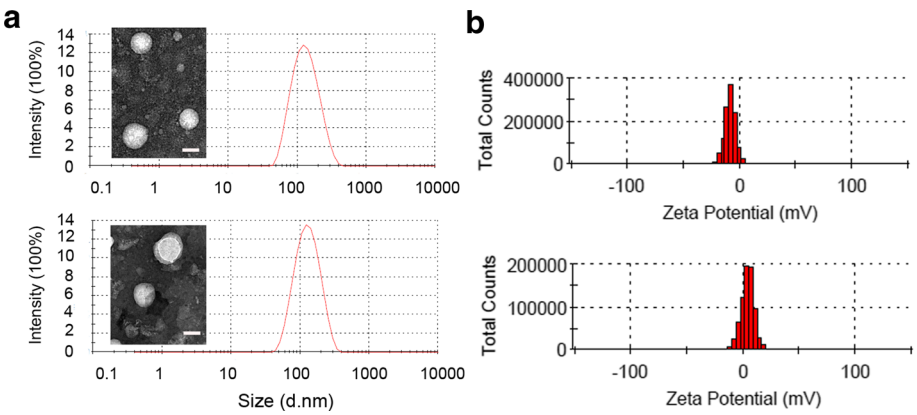

Fig. 1. Characterization of PTX/αGC-TH-Lip. **a** Size and morphology of PTX/αGC-TH-Lip at pH 7.4 and pH 6.0. Scale bar = 100 nm. **b** Zeta potential of PTX/αGC-TH-Lip at pH 7.4 and 6.0

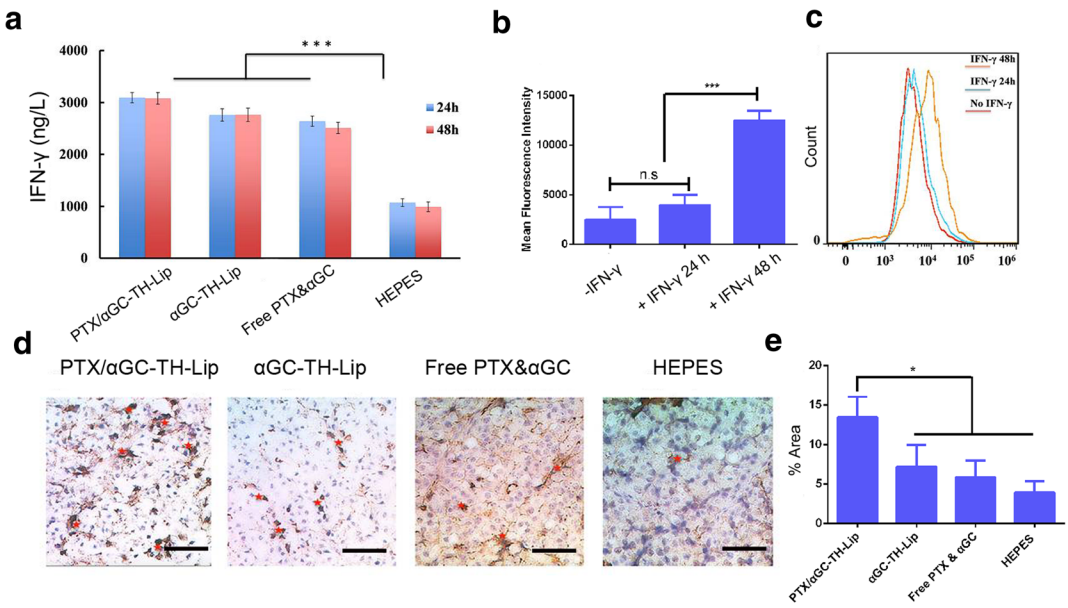

Fig. 2. The production of IFN-γ and expression of PD-L1 after treatment of different αGC preparations. **a** Serum IFN-γ levels in mice at 24 or 48 h after treatment with PTX/αGC-TH-Lip, αGC-TH-Lip, or free PTX plus αGC ($n = 3$, mean ± SD, ***$p < 0.005$). **b**, **c** The expression of PD-L1 on B16F10 cells in the presence of IFN-γ as analyzed by flow cytometry ($n = 3$, mean ± SD, ***$p < 0.005$, N.S, nonsignificant). **d** Immunohistochemical staining of PD-L1 in paraffin sections of B16F10 tumors after treatment with PTX/αGC-TH-Lip, αGC-TH-Lip, free PTX+αGC, or HEPES buffer ($n = 3$, scale bar = 50 μm). Proliferative cells shown in brown (red star). **e** Semiquantitative analysis of immunohistochemical staining of PD-L1. Six to ten random fields were quantified by the ImageJ software after appropriate thresholding. Data represent the percent of positive staining ($n = 6$–10, mean ± SD, *$p < 0.05$)

Based on these observations, IFN-γ was increased in PTX/αGC-TH-Lip-treated mice and consequently upregulated the PD-L1 expression in tumor cells. To identify the optimal interval of administration, the upregulation of PD-L1 in tumor cells was analyzed at 24 or 48 h after incubation with IFN-γ by staining with FITC-labeled PD-L1 antibody. As shown in Fig. 2b, c, no significant upregulation of PD-L1 was observed in tumor cells at 24 h post-treatment, while PD-L1 expression was three times higher compared with cells without IFN-γ at 48 h ($p < 0.01$), suggesting that PD-L1 antibody should be given at 48 h post-PTX/αGC-TH-Lip administration. Furthermore, the in vivo upregulation of PD-L1 was also assessed in tumor-bearing mice treated with PTX/αGC-TH-Lip by paraffin sections followed by immunohistochemistry staining (Fig. 2d, e). The PD-L1 level was obviously higher in mice treated with PTX/αGC-TH-Lip than in those treated with αGC-TH-Lip or free PTX and αGC, probably owing to the higher activation of T cells and NK cell responses and enhanced IFN-γ levels in PTX/αGC-TH-Lip-treated mice (Fig. 2d). The semiquantitative analysis by ImageJ indicated that the percent of positive area of PTX/αGC-TH-Lip-treated group was significantly higher than other groups (Fig. 2e). Though PTX/αGC-TH-Lip exhibited increased tumor inhibition, the upregulation of PD-L1 in tumor cells might in turn hamper the anti-tumor immune responses.

PD-L1 Enhanced the Anti-Tumor Responses of PTX/αGC-TH-Lip

Parameters including size, charge, and surface modifications affect the drug accumulation in tumors. Liposomal drug delivery systems utilize the enhance permeation and retention (EPR) effect of tumor tissues to enhance the tumor-targeted delivery. Moreover, pegylated liposome prolongs the blood circulation and further enhances the drug accumulation in tumors (28). In comparison, non-liposomal formulation could not take advantage of the EPR effect, which yielded poor tumor targeting. In our previous research, we have analyzed the biodistribution of TH-Lip and PEG-Lip. The results indicated that TH-Lip further elevated the drug accumulation compared with PEG-Lip (11). Tumor cells that escape immunosurveillance usually express molecules to suppress the anti-tumor immune responses, such as PD-L1/PD-1 (29), indoleamine 2,3-dioxygenase (IDO) (30), and transforming growth factor-β (TGF-β) (31). Generally, PD-1 is expressed on the surface of various immune cells, including activated T cells, NK cells, macrophages, dendritic cells, and B cells. Upon the initiation of immune responses, the activation of T cells further induced the expression of PD-1 on naive T cells, impairing the T cell functions in turn and consequently facilitating tumor escape (32). This process was associated with the expression of additional inhibitory receptors, such as T cell immunoglobulin mucin 3 (Tim-3) or lymphocyte activation gene 3 protein (LAG-3) (33,34). The interaction between PD-1 and its ligand PD-L1 formed a "check point" for anti-tumor immune responses. The upregulation of PD-L1 after treatment with PTX/αGC-TH-Lip may compromise the cytotoxicity of immunotherapy. In our pilot study, the optimal interval between PTX/αGC-TH-Lip and PD-L1 antibodies was determined to be 48 h (Supporting Information Fig. S4). After successful establishment of B16F10 melanoma, mice received 3 cycles of administration via the tail vein (Fig. 3a), and the tumor volume was monitored every other day. The combination of PD-L1 antibody significantly inhibited tumor growth compared with PTX/αGC-TH-Lip (Fig. 3b, $p < 0.05$).

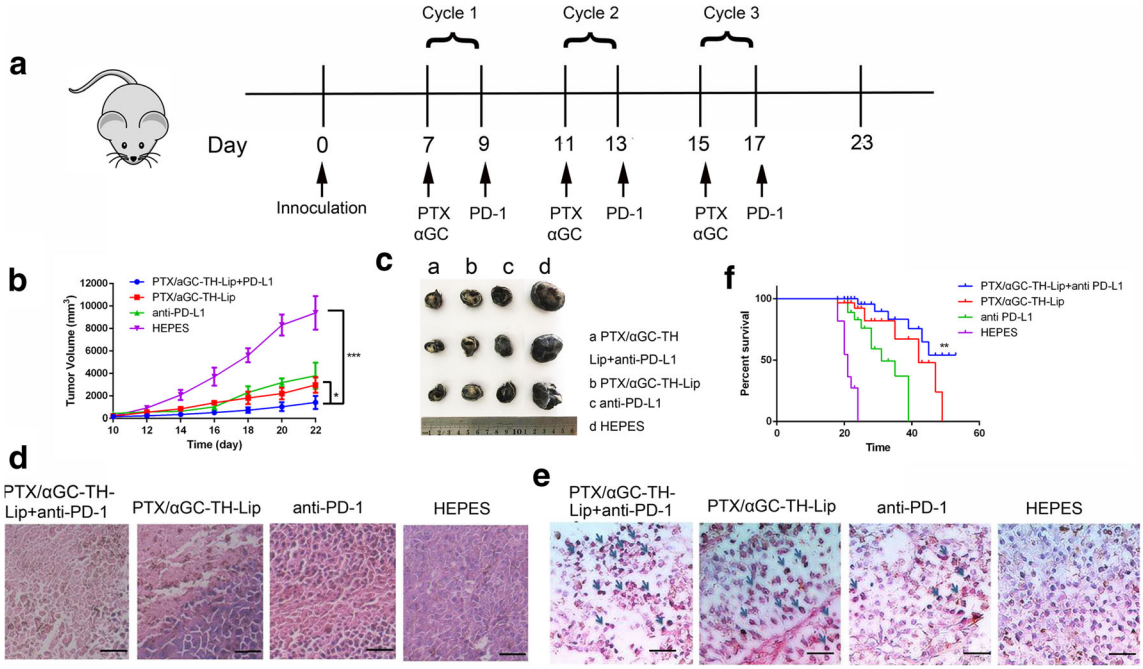

Fig. 3. The anti-tumor effects of PTX/αGC-TH-Lip combined with PD-L1 antibody. **a** Administration regimen of anti-tumor experiments. The B16F10 melanoma xenograft mouse model was established on day 0. Mice received PTX/αGC-TH-Lip by i.v. injection 7 days post-inoculation, followed by PD-L1 antibody administration 48 h later. After 3 cycles of administration, mice were sacrificed on day 23. **b** Tumor volume and **c** representative tumor images of mice receiving different treatments ($n = 7$, mean ± SD, $^{*}p < 0.05$, $^{***}p < 0.005$). **d** H&E staining of tumor tissues after different treatments. Scale bars = 50 μm. **e** TUNEL staining (apoptotic and necrotic cells are shown in red) of tumor tissues from mice treated with different preparations. **f** The survival curves of B16F10 melanoma tumor-bearing mice after different treatments ($n = 10$, $^{**}p < 0.01$)

The tumor growth curve of individual animal was shown in Supporting Information Fig. S5. The images of tumors isolated from tumor-bearing mice also confirmed the tumor inhibition effect of combined therapy (Fig. 3c). Subsequently, the tumor tissues were subjected to paraffin sectioning followed by H&E and TUNEL staining. As shown in Fig. 3d, obvious necrosis and nuclear shrinkage were observed in the combination therapy group. In comparison, PTX/αGC-TH-Lip-treated mice or single anti-PD-L1 antibody-treated mice showed less necrosis, indicating that combined therapy was superior in inducing tumor cell necrosis. Furthermore, TUNEL staining also indicated that the combined therapy induced obvious apoptosis in tumor cells (Fig. 3e). The semiquantitative results of TUNEL staining were shown in Supporting Information Fig. S6. The positive area of combined therapy was significantly higher than that of PTX/αGC-TH-Lip, anti-PD-L1, and HEPES-treated mice. The enhanced anti-tumor effects further led to prolonged survival time. As shown in Fig. 3f, mice receiving combined therapy exhibited the longest survival time (up to over 50 days, $p < 0.01$). The combination of PD-L1 antibody significantly elevated the anti-melanoma effect of PTX/αGC-TH-Lip.

Though PD-L1 inhibition has shown promising results and has been used as a first-line treatment in various cancers such as metastatic melanoma, the effectiveness of a single PD-1 or PD-L1 antibody is still not satisfactory. Anti-PD-L1 monotherapy reportedly remains ineffective in more than 60% of cancer patients (22). Multiple strategies have been combined with checkpoint inhibitors, many of which have entered clinical trials (23,35). Inhibition of regulatory T cells (Tregs) or blocking the inhibition of NK cells may strengthen the anti-tumor responses of PD-L1 antibody and improve the duration of response by stimulating the memory T cells (36,37). In our previous research, chemotherapy using PTX and immunoadjuvant αGC successfully initiated anti-tumor immune responses and inhibited tumor growth. The combination of PD-L1 antibody and PTX/αGC-TH-Lip not only strengthened the effect of PD-L1 antibody but also inhibited further tumor growth.

Notably, in the present manuscript, we adopted a therapeutic chemoimmunotherapy to inhibit the growth of B16F10 xenograft, which is a highly aggressive tumor model. Complete tumor elimination is usually observed in preventive strategies such as tumor vaccination or CAR-T therapies (38,39). Since our hypothesis is based on an established tumor model, it may be hard to achieve complete elimination of tumor. Nevertheless, from the tumor volume results, it can be seen that the tumor volume of combined therapy was significantly higher than PTX/αGC-TH-Lip-treated group (Fig. 3b, $p < 0.05$). The combined therapy also showed a significantly higher positive TUNEL staining than PTX/αGC/TH-Lip, anti-PD-L1, and HEPES groups ($^{*}p < 0.05$, $^{***}p < 0.005$). The results indicated that the combined therapy significantly increased the apoptosis of tumor cells. The anti-tumor experiment was repeated twice to ascertain the results.

PD-L1 Antibody Elevated the Anti-Metastatic Effect of PTX/αGC-TH-Lip

The initiation of the anti-tumor immune response is capable of inhibiting the metastasis of tumor cells (40). The anti-metastatic effect of the combined therapy was analyzed in a B16F10 lung

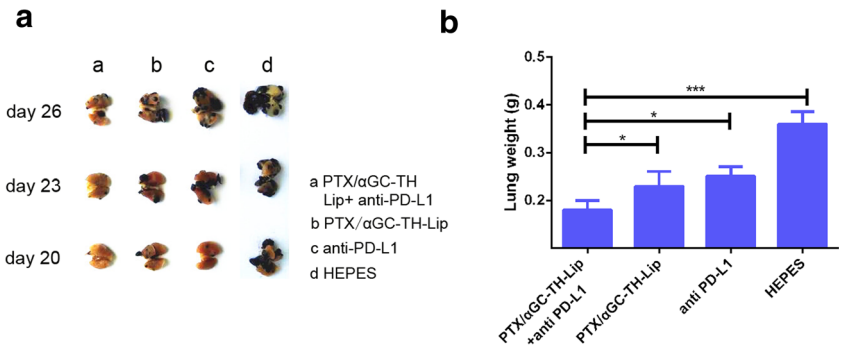

Fig. 4. The anti-metastatic effects of PTX/αGC-TH-Lip combined with PD-L1 on the experimental lung metastasis model of B16F10 melanoma. The melanoma lung metastasis mouse model was established by i.v. injection of B16F10 cells. **a** The metastatic nodules in the lungs after different treatments. The lung tissues were collected at day 20, day 23, and day 26. **b** The weight of lungs collected from each treated group at day 26 ($n = 3$, mean ± SD, $^{*}p < 0.05$, $^{***}p < 0.005$)

metastasis model. As shown in Fig. 4a, at day 20 and day 23, no obvious metastasis nodules were observed in the combined therapy-treated mice. Even at day 26, only slight nodules were seen. In comparison, mice treated with PTX/αGC-TH-Lip or anti-PD-L1 antibody alone showed a higher metastasis rate. The lung weight results showed similar trend. After treatment with combination therapy, lung metastasis was significantly alleviated (Fig. 4b, $p < 0.05$).

Previous researches have studied the relationship between metastasis and PD-L1 expression, and epithelial-to-mesenchymal transition (EMT) has been reported to be related to T cell dysfunction. PD-L1 is a downstream target of the miR-200/ZEB1 axis, and the EMT activator ZEB1 upregulates PD-L1 via the microRNA 200/ZEB1 axis (41,42). Furthermore, in clinical trials, the blockade of PD-L1 by antibodies suppresses metastatic diseases in lung cancer patients (43). In our previous research, the coadministration of chemotherapy and immunoadjuvant αGC repressed the lung metastasis of B16F10 melanoma. After combination therapy with the PD-L1 antibody, the anti-metastatic effect of PTX/αGC-TH-Lip was further promoted.

PD-L1 Antibody Enhanced the *Ex Vivo* CTL Response

In vivo anti-tumor and anti-metastasis investigations have revealed the potency of PTX/αGC-TH-Lip and PD-L1 antibodies, which proved the tumor growth inhibition and lung metastasis suppression of this combined strategy. These effects are mainly attributed to the enhanced cytotoxic T cell responses and the alleviated immunosuppression mediated by PD-L1 antibody. To prove this concept, we conducted an *ex vivo* CTL analysis. $CD8^+$ T cells were isolated from mice that received two administrations dual drug-loaded liposomes. After stimulation with IL-2, the effector cells were added into preseeded B16F10 or C26 cells at different ratios. PD-L1 antibody was added to effector cells obtained from mice treated with PTX/αGC-TH-Lip to evaluate the promotion of CTL cytotoxicity. The cytotoxicity of CTL was evaluated by an LDH assay. As shown in Fig. 5a, the addition of PD-L1 antibody significantly promoted the CTL responses when the *E*/*T* ratio was 20:1 ($p < 0.01$) and 5:1 ($p < 0.05$). In comparison, no significant difference in CTL responses was observed when the *E*/*T* ratio was 1:1, indicating that the PD-L1 antibody itself could not induce the cytotoxic lysis of $CD8^+$ T cells. The promotion of CTL responses is mainly attributed to the relief of immunosuppressive signals mediated by PD-L1 antibody. Irrelevant C26 cells were used as control cells. $CD8^+$ T cells isolated from PTX/αGC-TH-Lip-treated mice could not induce specific lysis on C26 cells, even after the addition of PD-L1 antibody. These results suggest that the cytotoxic T cell responses are antigen-specific (Fig. 5b).

The Combination of PD-L1 Enhances the Adoptive T Cell Therapy

The *ex vivo* CTL responses revealed that the PD-L1 antibody was capable of elevating the anti-tumor immune responses. To confirm the in vivo T cell response promotion

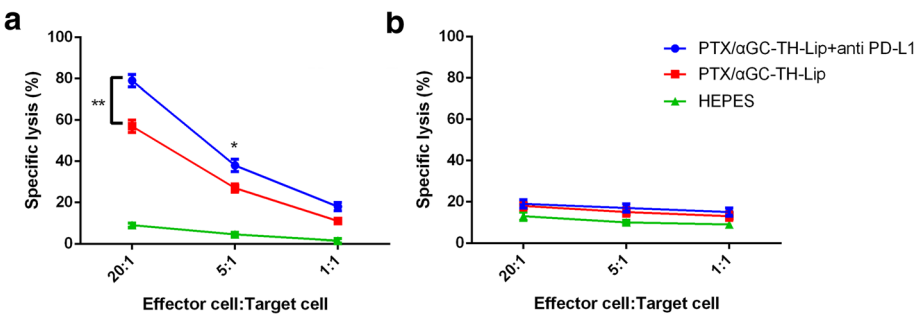

Fig. 5. The cytotoxicity assay of $CD8^+$ T lymphocytes against **a** B16F10 cells and **b** C26 cells ($n = 3$, mean ± SD, $^{*}p < 0.05$, $^{**}p < 0.01$)

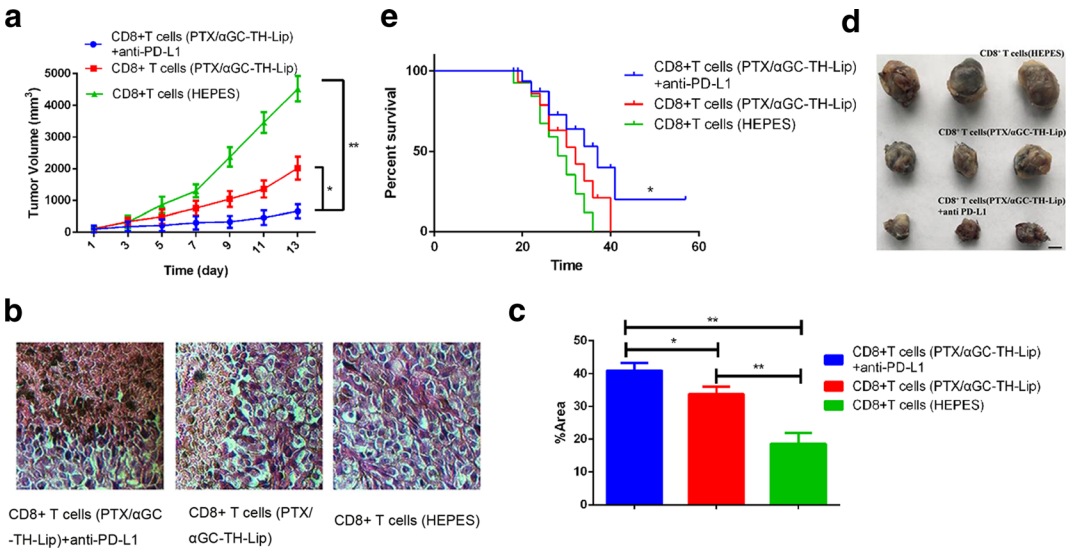

Fig. 6. The adoptive immunotherapy with CD8$^+$ T cells in combination with PD-L1 antibody. **a** Tumor growth curve of mice treated with CD8$^+$ cells obtained from HEPES- or PTX/αGC-TH-Lip-treated mice. PD-L1 antibody was administered intraperitoneally at a dose of 5 mg/kg ($n = 5$, mean ± SD, $^*p < 0.05$, $^{**}p < 0.01$). **b** H&E staining of tumor tissues from different treatment groups. **c** Semiquantitative analysis of H&E staining. Six to ten random fields were quantified by the ImageJ software after appropriate thresholding. Data represent the percent of apoptotic area ($n = 6$–10, mean ± SD, $^*p < 0.05$, $^{**}p < 0.01$). **d** Representative images of tumors from each group. Scale bars = 1 cm. **e** The survival curves of B16F10 melanoma tumor-bearing mice after different treatments ($n = 10$, $^*p < 0.05$)

of PD-L1, adoptive T cell therapy was conducted. CD8$^+$ T cells were isolated from mice treated with PTX/αGC-TH-Lip or HEPES buffer and were subsequently injected into tumor-bearing mice. In addition, PD-L1 antibody was combined with CD8$^+$ T cells obtained from PTX/αGC-TH-Lip to analyze the in vivo promotion of CTL responses. As shown in Fig. 6a, mice treated with CD8$^+$ T cells isolated from PTX/αGC-TH-Lip-treated mice significantly inhibited tumor growth; furthermore, the combination of PD-L1 antibody dramatically suppressed tumor growth (Fig. 6a, $p < 0.01$, $p < 0.05$). H&E staining of tumor sections indicated that the combination of PD-L1 antibody and CD8$^+$ T cells isolated from PTX/αGC-TH-Lip-treated mice induced obvious apoptosis of tumor cells (Fig. 6b). The semiquantitative analysis by ImageJ also indicated that PD-L1 antibody promoted the cytotoxicity of CD8$^+$ T cells from PTX/αGC-TH-Lip-treated mice (Fig. 6c, $p < 0.05$). The images of tumors isolated from tumor-bearing mice also reflected the enhanced anti-tumor immune responses of the combined therapy (Fig. 6d). In addition, we studied the survival time of mice treated with adoptive T cell therapy. Consistent with the above results, PD-L1 antibody plus CD8$^+$ T cells from PTX/αGC-TH-Lip-treated melanoma-bearing mice exhibited a longer survival (median survival time of over 35 days). In comparison, the median survival time of mice treated with CD8$^+$ T cells isolated from HEPES-treated mice and PTX/

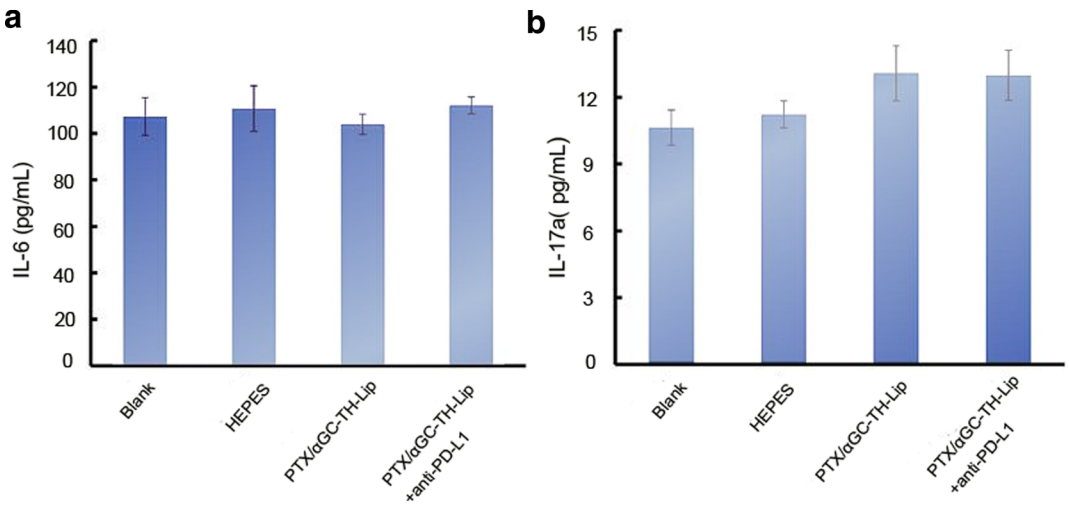

Fig. 7. The in vivo secretion of cytokines after treatment with HEPES buffer, PTX/αGC-TH-Lip, or PTX/αGC-TH-Lip combined with PD-L1 antibody. **a** IL-6 levels in serum. **b** IL-17a levels in serum after different treatments ($n = 5$, mean ± SD)

αGC-TH-Lip-treated mice was 25 and 30 days, respectively (Fig. 6e, $p < 0.05$). These observations confirmed the promotion of CTL responses by the PD-L1 antibody.

Adoptive T cell therapy, which includes *in vitro* expanded peripheral blood, tumor-infiltrating T lymphocytes, and genetically engineered chimeric antigen receptor T cells, has exhibited great potential in immunotherapy. Nevertheless, the PD-1 level in adoptive T cells has been shown to be upregulated, which may hamper the therapeutic effects (33,44). Therefore, considering the upregulation of PD-L1 and PD-1 in tumor cells and APCs after immune activation, it is assumed that concurrent or post-PD pathway blockade in adoptive T cell therapy may improve the functionality of the transferred T cells (25). Feldman *et al.* showed that the downregulation of PD-L1 on tumor-infiltrating cells increased the function of effector cells and elevated the polyfunctional cytokine profile (45). Herein, in our present manuscript, PD-L1 antibody further improved the anti-tumor effects of $CD8^+$ T cells isolated from PTX/αGC-TH-Lip-treated mice, supporting the benefit of a combination of adoptive T cell therapy and PD pathway blockade.

Preliminary Safety Analysis of the Combined Therapy

The activation of non-specific immunity may cause unwanted side effects or even autoimmune diseases. Therefore, it is essential to study the production of inflammatory cytokines and the safety of healthy organs. T helper 17 (T_H 17) cells play important roles in inflammation and autoimmune diseases and secrete T_H17 effector cytokines such as IL-17a, which in turn induce the secretion of proinflammatory cytokines such as IL-6, thereby regulating tissue inflammation, and damage (46). After three administrations, the production of IL-6 and IL-17a in serum was analyzed. As shown in Fig. 7a, b, cytokines from mice treated with HEPES, PTX/αGC-TH-Lip, or PTX/αGC-TH-Lip plus PD-L1 antibody were at the same level. This result suggested that the cytokines and immune responses induced by PTX/αGC-TH-Lip and PD-L1 were antigen-specific and did not cause obvious inflammation at the given dosage. The preliminary safety assessment was conducted by the sectioning and H&E staining of major organs (Supporting Information Fig. S7). No histological changes were seen in the major organs of tumor-bearing mice, indicating that the chemoimmunotherapy has good safety and biocompatibility.

CONCLUSION

In the present study, we designed a tumor-targeted chemoimmunotherapeutic strategy using a combination of PD-L1 antibody and PTX/αGC coloaded TH peptide-modified liposomes to relieve the immunosuppressive effects in melanoma treatment. First, we confirmed that the administration of PTX/αGC-TH-Lip upregulated the IFN-γ level in the body, which in turn increased the expression of PD-L1 on tumor cells. The subsequent inhibition of PD-L1 promoted the anti-tumor effects of PTX/αGC-TH-Lip by elevating the magnitude of the immune responses. In addition, PD-L1 antibody also enhanced the anti-metastatic effect of PTX/αGC-TH-Lip. The *in vitro* mechanism study revealed that the elevated anti-tumor and anti-metastatic effects were probably owing to the enhanced CTL responses. Moreover, the combined strategy did not induce obvious side effects. The combination of PD-L1 antibody and chemoimmunotherapy has proven to be a promising strategy for metastatic melanoma treatment.

FUNDING

We acknowledge the financial support of the National Natural Science Foundation of China (Nos. 81690261 and 81703450) and the Fundamental Research Funds for Central Universities (2018SCU12026, the Postdoctoral Foundation of Sichuan University).

COMPLIANCE WITH ETHICAL STANDARDS

Conflict of Interest The authors declare that they have no conflict of interest

REFERENCES

1. Barker HE, Paget JTE, Khan AA, Harrington KJ. The tumour microenvironment after radiotherapy: mechanisms of resistance and recurrence. Nat Rev Cancer. 2015;15:409–25.
2. Cook AM, Lesterhuis WJ, Nowak AK, Lake RA. Chemotherapy and immunotherapy: mapping the road ahead. Curr Opin Immunol. 2016;39:23–9.
3. Kepp O, Senovilla L, Vitale I, Vacchelli E, Adjemian S, Agostinis P, et al. Consensus guidelines for the detection of immunogenic cell death. OncoImmunology. 2014;3(9):e955691.
4. Steinhagen F, Kinjo T, Bode C, Klinman DM. TLR-based immune adjuvants. Vaccine. 2011;29(17):3341–55.
5. Parmiani G, Castelli C, Pilla L, Santinami M, Colombo MP, Rivoltini L. Opposite immune functions of GM-CSF administered as vaccine adjuvant in cancer patients. Ann Oncol. 2007;18(2):226–32.
6. Rosenberg SA. IL-2: the first effective immunotherapy for human cancer. J Immunol. 2014;192(12):5451–8.
7. Li M, Zhao M, Fu Y, Li Y, Gong T, Zhang Z, et al. Enhanced intranasal delivery of mRNA vaccine by overcoming the nasal epithelial barrier via intra- and paracellular pathways. J Control Release. 2016;228:9–19.
8. Li M, Li Y, Peng K, Wang Y, Gong T, Zhang Z, et al. Engineering intranasal mRNA vaccines to enhance lymph node trafficking and immune responses. Acta Biomater. 2017;64:237–48.
9. Subrahmanyam PB, Webb TJ. Boosting the immune response: the use of iNKT cell ligands as vaccine adjuvants. Front Biol. 2012;7(5):436–44.
10. Shi S, Zhou M, Li X, Hu M, Li C, Li M, et al. Synergistic active targeting of dually integrin αvβ3/CD44-targeted nanoparticles to B16F10 tumors located at different sites of mouse bodies. J Control Release. 2016;235:1–13.
11. Yang Y, Tai X, Shi K, Shaobo R, Qiu Y, Zhang Z, et al. A new concept of enhancing immuno-chemotherapeutic effects against B16F10 tumor via systemic administration by taking advantages of the limitation of EPR effect. Theranostics. 2016;6(12):2141–60.
12. Topalian SL, Drake CG, Pardoll DM. Targeting the PD-1/B7-H1(PD-L1) pathway to activate anti-tumor immunity. Curr Opin Immunol. 2012;24(2):207–12.
13. Gros A, Robbins PF, Yao X, Li YF, Turcotte S, Tran E, et al. PD-1 identifies the patient-specific CD8+ tumor-reactive repertoire infiltrating human tumors. J Clin Invest. 2014;124(5):2246–59.

14. Yokosuka T, Takamatsu M, Kobayashi-Imanishi W, Hashimoto-Tane A, Azuma M, Saito T. Programmed cell death 1 forms negative costimulatory microclusters that directly inhibit T cell receptor signaling by recruiting phosphatase SHP2. J Exp Med. 2012;209(6):1201–17.
15. Mahoney KM, Rennert PD, Freeman GJ. Combination cancer immunotherapy and new immunomodulatory targets. Nat Rev Drug Discov. 2015;14:561.
16. Seung-Jin L, Byeong-Churl J, Soo-Woong L, Young-Il Y, Seong-Il S, Yeong-Min P, et al. Interferon regulatory factor-1 is prerequisite to the constitutive expression and IFN-γ-induced upregulation of B7-H1 (CD274). FEBS Lett. 2006;580(3):755–62.
17. Taube JM, Anders RA, Young GD, Xu H, Sharma R, McMiller TL, et al. Colocalization of inflammatory response with B7-H1 expression in human melanocytic lesions supports an adaptive resistance mechanism of immune escape. Sci Transl Med. 2012;4(127):127ra37-ra37.
18. Khalil DN, Smith EL, Brentjens RJ, Wolchok JD. The future of cancer treatment: immunomodulation, CARs and combination immunotherapy. Nat Rev Clin Oncol. 2016;13:273–90.
19. Robert C, Long GV, Brady B, Dutriaux C, Maio M, Mortier L, et al. Nivolumab in previously untreated melanoma without BRAF mutation. New Engl J Med. 2015;372(4):320–30.
20. Robert C, Schachter J, Long GV, Arance A, Grob JJ, Mortier L, et al. Pembrolizumab versus ipilimumab in advanced melanoma. New Engl J Med. 2015;372(26):2521–32.
21. Rizvi NA, Mazières J, Planchard D, Stinchcombe TE, Dy GK, Antonia SJ, et al. Activity and safety of nivolumab, an anti-PD-1 immune checkpoint inhibitor, for patients with advanced, refractory squamous non-small-cell lung cancer (CheckMate 063): a phase 2, single-arm trial. Lancet Oncol. 2015;16(3):257–65.
22. Simon S, Labarriere N. PD-1 expression on tumor-specific T cells: friend or foe for immunotherapy? OncoImmunology. 2018;7(1):e1364828.
23. Antonia SJ, Brahmer JR, Gettinger S, Chow LQ, Juergens R, Shepherd FA, et al. Nivolumab (anti-PD-1; BMS-936558, ONO-4538) in combination with platinum-based doublet chemotherapy (PT-DC) in advanced non-small cell lung cancer (NSCLC). Int J Radiat Oncol Biol Phys. 2014;90(5):–S2.
24. Amin A, Plimack ER, Infante JR, Ernstoff MS, Rini BI, McDermott DF, et al. Nivolumab (anti-PD-1; BMS-936558, ONO-4538) in combination with sunitinib or pazopanib in patients (pts) with metastatic renal cell carcinoma (mRCC). J Clin Oncol. 2014;32(15_suppl):5010.
25. Zou W, Wolchok JD, Chen L. PD-L1 (B7-H1) and PD-1 pathway blockade for cancer therapy: mechanisms, response biomarkers, and combinations. Sci Transl Med. 2016;8(328):328rv4-rv4.
26. Zou W, Chen L. Inhibitory B7-family molecules in the tumour microenvironment. Nat Rev Immunol. 2008;8:467–77.
27. Fujii S-I, Shimizu K, Kronenberg M, Steinman RM. Prolonged IFN-γ-producing NKT response induced with α-galactosylceramide-loaded DCs. Nat Immunol. 2002;3:–867.
28. Torchilin VP. Recent advances with liposomes as pharmaceutical carriers. Nat Rev Drug Discov. 2005;4:145–60.
29. Chen L, Han X. Anti–PD-1/PD-L1 therapy of human cancer: past, present, and future. J Clin Invest. 2015;125(9):3384–91.
30. Mellor AL, Munn DH. Ido expression by dendritic cells: tolerance and tryptophan catabolism. Nat Rev Immunol. 2004;4:762–74.
31. Mangan PR, Harrington LE, O'Quinn DB, Helms WS, Bullard DC, Elson CO, et al. Transforming growth factor-β induces development of the TH17 lineage. Nature. 2006;441:231–4.
32. Liu Y, Yu Y, Yang S, Zeng B, Zhang Z, Jiao G, et al. Regulation of arginase I activity and expression by both PD-1 and CTLA-4 on the myeloid-derived suppressor cells. Cancer Immunol Immunother. 2009;58(5):687–97.
33. Fourcade J, Sun Z, Benallaoua M, Guillaume P, Luescher IF, Sander C, et al. Upregulation of Tim-3 and PD-1 expression is associated with tumor antigen-specific CD8+ T cell dysfunction in melanoma patients. J Exp Med. 2010;207(10):2175–86.
34. Chauvin J-M, Pagliano O, Fourcade J, Sun Z, Wang H, Sander C, et al. TIGIT and PD-1 impair tumor antigen-specific CD8+ T cells in melanoma patients. J Clin Invest. 2015;125(5):2046–58.
35. Frederick DT, Piris A, Cogdill AP, Cooper ZA, Lezcano C, Ferrone CR, et al. BRAF inhibition is associated with enhanced melanoma antigen expression and a more favorable tumor microenvironment in patients with metastatic melanoma. Clin Cancer Res. 2013;19(5):1225–31.
36. Chretien A-S, Le Roy A, Vey N, Prebet T, Blaise D, Fauriat C, et al. Cancer-induced alterations of NK-mediated target recognition: current and investigational pharmacological strategies aiming at restoring NK-mediated anti-tumor activity. Front Immunol. 2014;5(122).
37. Woo S-R, Turnis ME, Goldberg MV, Bankoti J, Selby M, Nirschl CJ, et al. Immune inhibitory molecules LAG-3 and PD-1 synergistically regulate T cell function to promote tumoral immune escape. Cancer Res. 2012;72(4):917–27.
38. Wu MR, Zhang T, DeMars LR, Sentman CL. B7H6-specific chimeric antigen receptors lead to tumor elimination and host anti-tumor immunity. Gene Ther. 2015;22:675–84.
39. Mansour M, Pohajdak B, Kast WM, Fuentes-Ortega A, Korets-Smith E, Weir GM, et al. Therapy of established B16-F10 melanoma tumors by a single vaccination of CTL/T helper peptides in VacciMax®. J Transl Med. 2007;5(1):20.
40. Ming Y, Li Y, Xing H, Luo M, Li Z, Chen J, et al. Circulating tumor cells: from theory to nanotechnology-based detection. Front Pharmacol. 2017;8(114):35.
41. Krebs AM, Mitschke J, Lasierra Losada M, Schmalhofer O, Boerries M, Busch H, et al. The EMT-activator Zeb1 is a key factor for cell plasticity and promotes metastasis in pancreatic cancer. Nat Cell Biol. 2017;19:518–29.
42. Chen L, Gibbons DL, Goswami S, Cortez MA, Ahn Y-H, Byers LA, et al. Metastasis is regulated via microRNA-200/ZEB1 axis control of tumour cell PD-L1 expression and intratumoral immunosuppression. Nat Commun. 2014;5:5241.
43. Brahmer JR. Harnessing the immune system for the treatment of non-small-cell lung cancer. J Clin Oncol. 2013;31(8):1021–8.
44. Matsuzaki J, Gnjatic S, Mhawech-Fauceglia P, Beck A, Miller A, Tsuji T, et al. Tumor-infiltrating NY-ESO-1-specific CD8+ T cells are negatively regulated by LAG-3 and PD-1 in human ovarian cancer. Proc Natl Acad Sci. 2010;107(17):7875–80.
45. Twyman-Saint Victor C, Rech AJ, Maity A, Rengan R, Pauken KE, Stelekati E, et al. Radiation and dual checkpoint blockade activate non-redundant immune mechanisms in cancer. Nature. 2015;520:373–7.
46. Miossec P, Kolls JK. Targeting IL-17 and TH17 cells in chronic inflammation. Nat Rev Drug Discov. 2012;11:763.